

CERN-TH/96-310  
RAL-96-092  
October 1996  
hep-ph/9611218

## Direct $J/\psi$ and $\psi'$ Polarization and Cross Sections at the Tevatron

MARTIN BENEKE<sup>1</sup> and MICHAEL KRÄMER<sup>2</sup>

<sup>1</sup>*Theory Division, CERN,  
CH-1211 Geneva 23, Switzerland*

<sup>2</sup>*Rutherford Appleton Laboratory,  
Chilton, Didcot, OX11 0QX, England*

### Abstract

Transverse polarization of  $^3S_1$  charmonium states, produced directly in  $p\bar{p}$  collisions at asymptotically large transverse momentum  $p_t$ , has emerged as the most prominent test of color octet contributions and spin symmetry in quarkonium production. We present predictions for the polar angle distribution at moderate values of  $p_t \sim 4 - 20$  GeV, covered by the Tevatron Run I data. We update the fits of NRQCD matrix elements and discuss their theoretical uncertainties. With our best fit values, no transverse polarization is expected at  $p_t \sim 5$  GeV, but the angular distribution is predicted to change dramatically as  $p_t$  increases to 20 GeV.

PACS numbers: 14.40.Gx, 13.88.+e, 13.85.Ni

During the past three years, the phenomenology of quarkonium production has undergone a phase of exciting developments. These followed from the application of Non-Relativistic QCD (NRQCD) [1], an effective theory that disentangles physics on the scale of the heavy quark mass  $m_Q$ , relevant to the production of a heavy quark pair, from physics on the scale of the bound state's binding energy  $m_Q v^2$ , relevant to the formation of the quarkonium. Inclusive quarkonium production is now viewed as a two-step process, where the production of a heavy quark pair  $Q\bar{Q}[n]$  in a certain angular momentum and color state  $n$  is described by a perturbatively calculable short-distance cross section  $d\hat{\sigma}_n$  and the subsequent quarkonium formation is parametrized by a nonperturbative matrix element  $\langle \mathcal{O}_n^\psi \rangle$ , which is subject to the power counting rules of NRQCD.

For  $J/\psi$  and  $\psi'$  (collectively denoted by  $\psi$ ) only the color singlet  $n = {}^3S_1^{(1)}$  intermediate state contributes at lowest order in the non-relativistic velocity expansion in  $v^2$ . (We use spectroscopic notation with the superscript in brackets denoting the color state.) Three more nonperturbative parameters, related to color octet configurations  $n = {}^3S_1^{(8)}, {}^1S_0^{(8)}, {}^3P_J^{(8)}$  appear as  $v^4$ -corrections. Their importance for  $\psi$  production has been understood in [2]. Because gluons couple easily to  ${}^3S_1$  octet states, gluon fragmentation into color octet quark pairs appears as the most plausible explanation of the large direct  $\psi$  production cross section observed at the Tevatron [3]. Subsequent to this observation many charmonium production processes have been reconsidered to gauge the impact of color octet contributions and to determine the corresponding nonperturbative matrix elements. (For reviews and references see [4].) Among the specific predictions of NRQCD, transverse polarization of direct  $\psi$  (i.e. not from  $B$  and  $\chi_c$  decays) at large transverse momentum  $p_t$  in  $p\bar{p}$  collisions at the Tevatron has emerged as the most distinct and most accessible signature [5, 6]. Transverse polarization also discriminates NRQCD from other approaches, like the color evaporation model which, in its most naive version, predicts the quarkonium to be produced unpolarized. At moderate  $p_t$  the polarization signature provides an important consistency check on the relative weight of the intermediate color octet states inferred from the unpolarized differential cross section.

Transverse polarization at large  $p_t$  is a direct consequence of gluon fragmentation as well as spin symmetry of the leading order NRQCD effective lagrangian. When  $p_t \gg 2m_c$  the fragmenting gluon is effectively on-shell

and transverse. The  $c\bar{c}$  pair in the color octet  ${}^3S_1$  state inherits the gluon's transverse polarization and so does the  $\psi$ , because the emission of soft gluons during hadronization does not flip the spin. Both, corrections due to spin-symmetry breaking and higher order fragmentation contributions have been estimated to be rather small [6]. However, the color octet  ${}^1S_0^{(8)}$  and  ${}^3P_J^{(8)}$  production channels, which do not have a fragmentation interpretation at leading order in the strong coupling  $\alpha_s$ , have large short-distance coefficients [7] and can dominate the  $p_t$ -distribution over a significant range of  $p_t$  covered by the present Tevatron data. The polarization yield from these subprocesses has not so far been calculated.

In this Letter we report on the calculation of all subprocesses for polarized direct  $\psi$  (not from  $B$  and  $\chi_c$  decays) production at leading order in  $\alpha_s$ . We update the extraction of NRQCD matrix elements from unpolarized cross sections first performed in [7] and discuss their uncertainties. The prediction for the polar angle distribution includes the higher order fragmentation corrections from [6] and covers the entire  $p_t$ -range  $p_t \sim 4 - 20$  GeV accessible with the Tevatron run I data. The polarization analysis of Tevatron data is under way [8].

The differential cross section for  $p\bar{p} \rightarrow \psi^{(\lambda)}(p_t) + X$  is given by

$$\frac{d\sigma}{dp_t} = \sum_{i,j} \int dx_1 dx_2 f_{i/p}(x_1) f_{j/\bar{p}}(x_2) \sum_n \frac{d\hat{\sigma}_{ij}^{(\lambda)}[n]}{dp_t} \langle \mathcal{O}_n^\psi \rangle, \quad (1)$$

where  $f_{i/p}$  and  $f_{j/\bar{p}}$  denote the parton densities and  $\lambda$  specifies the helicity state. At non-vanishing transverse momentum, the leading partonic subprocesses  $i + j \rightarrow c\bar{c}[n] + k$  occur at order  $\alpha_s^3$ . To obtain the short-distance cross section for a given  $c\bar{c}$  state  $n$ , we expand, in the rest frame of the heavy quark pair, the partonic amplitude in the relative momentum of the heavy quarks and decompose the amplitude in spin and color. The amplitude squared for  $i + j \rightarrow \psi^{(\lambda)} + X$  can now be written as

$$\mathcal{M} = \sum_n \mathcal{M}_{n;kl\dots}^{(\lambda)} \langle \mathcal{O}_{n;kl\dots}^{\psi^{(\lambda)}} \rangle, \quad (2)$$

where the sum is ordered as an expansion in  $v^2$ . The cartesian tensors

$$\langle \mathcal{O}_{n;kl\dots}^{\psi^{(\lambda)}} \rangle = \sum_X \langle 0 | \chi^\dagger \kappa_{n;k\dots} \psi | \psi^{(\lambda)} X \rangle \langle \psi^{(\lambda)} X | \psi^\dagger \kappa'_{n;l\dots} \chi | 0 \rangle \quad (3)$$

describe the nonperturbative transition of the  $c\bar{c}$  pair into a polarized quarkonium  $\psi$  and any number of light hadrons  $X$ . Up to  $v^6$ -corrections to the color singlet contribution, Lorentz decomposition of these tensors, together with spin symmetry, allows us to reduce the matrix elements to four nonperturbative parameters  $\langle\mathcal{O}_1^\psi(^3S_1)\rangle$ ,  $\langle\mathcal{O}_8^\psi(^3S_1)\rangle$ ,  $\langle\mathcal{O}_8^\psi(^1S_0)\rangle$ ,  $\langle\mathcal{O}_8^\psi(^3P_0)\rangle$ . They are defined in [1] and include a sum over polarizations  $\lambda$ . We do not consider color singlet operators such as  $\mathcal{P}_1^\psi(^3S_1)$ , in the notation of [1], whose contributions are expected to be irrelevant.

For unpolarized production, the calculational procedure sketched above leads to results identical to those obtained with the standard amplitude projection method [9]. The polarized production cross section, however, requires special care as interference contributions from intermediate  $c\bar{c}$  pairs in different angular momentum states  $JJ_z$  no longer cancel [6, 10, 11]. In this case, the relevant projections are unambiguously specified by rotational invariance and spin symmetry implemented in the decomposition of  $\langle\mathcal{O}_{n;kl\dots}^{\psi(\lambda)}\rangle$  and can be found in [6]. For the  $S = 0$ ,  $L = 0$  intermediate state, each helicity state contributes one third of the unpolarized cross section. For the  $P$ -wave intermediate state, one must first sum over all orbital angular momentum states  $L_z$  and then project with the polarization vector  $\epsilon(\lambda)$  of the quarkonium. The short-distance coefficients that enter  $d\hat{\sigma}_{ij}^{(\lambda)}[n]$  can now be written as

$$A_{ij}[n] + B_{ij}[n] (\epsilon(\lambda) \cdot k_1)^2 + C_{ij}[n] (\epsilon(\lambda) \cdot k_2)^2 + D_{ij}[n] (\epsilon(\lambda) \cdot k_1) (\epsilon(\lambda) \cdot k_2), \quad (4)$$

where  $k_1$  and  $k_2$  are the momenta of the initial state partons and  $ij = gg, gq, g\bar{q}, q\bar{q}$ . Detailed expressions for the coefficients  $A, \dots, D$  will be presented elsewhere. Summing over all polarizations  $\lambda$ , we find agreement with the unpolarized cross sections computed in [7].

The nonperturbative matrix elements  $\langle\mathcal{O}_n^\psi\rangle$  that enter the color octet contributions can be adjusted to fit the experimental data as shown in Figs. 1 and 2, where we compare the transverse momentum distributions for unpolarized direct  $J/\psi$  and  $\psi'$  production with the most recent CDF data [12] ( $\sqrt{s} = 1.8$  TeV).<sup>1</sup> At large  $p_t$ , the cross section is dominated by gluon fragmentation into color octet  $^3S_1$  charm pairs [2, 13]. We have resummed the

---

<sup>1</sup>For direct  $J/\psi$  production, indirect contributions from  $\chi$  decays are removed, but those from  $\psi'$  decays are included in both the data and theoretical prediction. The indirect  $\psi'$  contribution amounts to about 11% [12]. In accounting for this contribution, we assumed that it is independent of  $p_t$ .

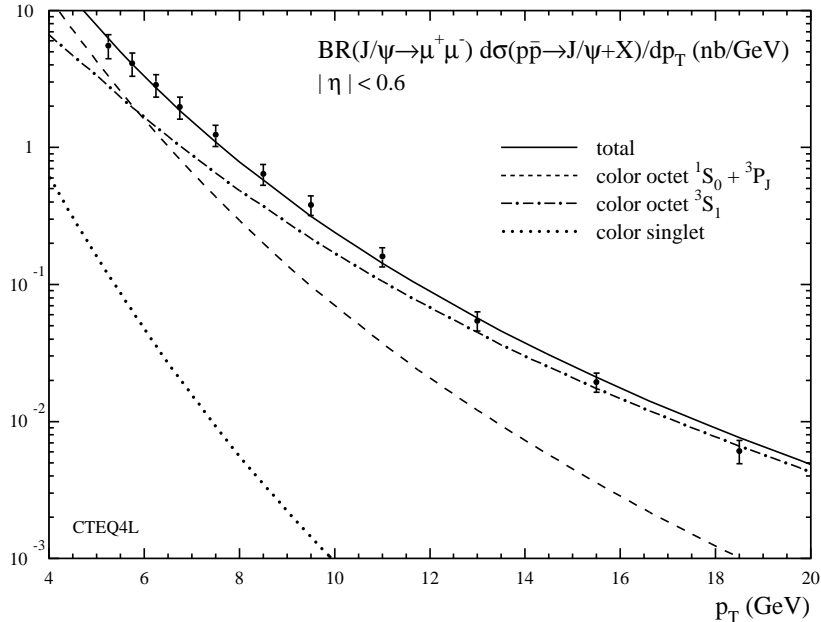


Figure 1: Fit of color octet contributions to direct  $J/\psi$  production data from CDF ( $\sqrt{s} = 1.8$  TeV, pseudorapidity cut  $|\eta| < 0.6$ ). The theoretical curves are obtained with CTEQ4L parton distribution functions, the corresponding  $\Lambda_4 = 235$  MeV, factorization scale  $\mu = (p_t^2 + 4m_c^2)^{1/2}$  and  $m_c = 1.5$  GeV. The fitted color octet matrix elements are given as the central values in Tab 1.

leading logarithms  $(\alpha_s \ln p_t^2 / (2m_c)^2)^n$  in this channel by solving the Altarelli-Parisi evolution equation for the corresponding fragmentation function. Evolution decreases the short-distance cross section and enhances the fitted value of  $\langle \mathcal{O}_8^\psi(^3S_1) \rangle$ . The color octet  $^1S_0$  and  $^3P_J$  channels are significant in the region  $p_t \lesssim 10$  GeV, but fall as  $d\hat{\sigma}/dp_t^2 \sim 1/p_t^6$  and become negligible for the unpolarized cross section at large  $p_t$ . Because the  $^1S_0^{(8)}$  and  $^3P_J^{(8)}$  short-distance cross sections have a similar  $p_t$  dependence, the transverse momentum distribution is sensitive only to a combination

$$M_k^\psi(^1S_0^{(8)}, ^3P_0^{(8)}) \equiv \langle \mathcal{O}_8^\psi(^1S_0) \rangle + \frac{k}{m_c^2} \langle \mathcal{O}_8^\psi(^3P_0) \rangle. \quad (5)$$

As  $p_t$  increases from 4 to 20 GeV,  $k$  varies from 3.9 to 3.0 for  $m_c = 1.5$  GeV. Since the  $^1S_0^{(8)}$  and  $^3P_J^{(8)}$  channels are significant only at low  $p_t$ , we choose

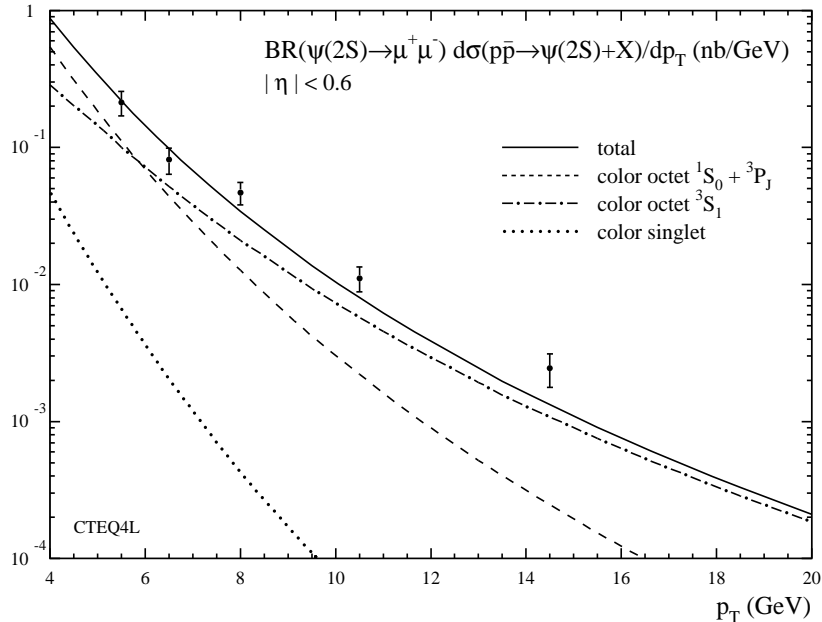


Figure 2: Same as Fig. 1 for prompt  $\psi'$  production.

$k = 3.5$ . [Note that  $k = 3$  was chosen in [7].] The theoretical prediction then depends on two phenomenological parameters.

As in [7], we fit these two parameters to the  $p_t$ -distribution, but attempt to estimate, at least partially, the theoretical uncertainties by varying the parton distribution function (PDF) set and renormalization (factorization) scale between  $1/2\sqrt{p_t^2 + 4m_c^2}$  and  $2\sqrt{p_t^2 + 4m_c^2}$ . The result is shown in Tab. 1 for three PDF sets [14], where the first error is statistical only and the second reflects the scale variation. In all cases the coupling  $\alpha_s(\mu)$  is evaluated according to the  $\Lambda_4$  specified by the chosen PDF set. In case of MRS(R2) this implies that  $\alpha_s(\mu)$  is evolved with two-loop accuracy.

While the value of  $\langle \mathcal{O}_8^\psi(^3S_1) \rangle$  is relatively stable with respect to the uncertainty related to the PDF, the fit of  $M_{3,5}^\psi(^1S_0^{(8)}, ^3P_0^{(8)})$  depends sensitively on all effects that modify the slope of the  $p_t$ -distribution, such as the small- $x$  behaviour of the gluon distribution or the evolution of the strong coupling. A steeper gluon distribution increases the slope of the  $p_t$ -distribution and leads to smaller values of  $M_{3,5}^\psi(^1S_0^{(8)}, ^3P_0^{(8)})$ . In addition, next-to-leading con-

	CTEQ4L	GRV (1994) LO	MRS(R2)
$\langle \mathcal{O}_8^{J/\psi}(^3S_1) \rangle$	$1.06 \pm 0.14_{-0.59}^{+1.05}$	$1.12 \pm 0.14_{-0.56}^{+0.99}$	$1.40 \pm 0.22_{-0.79}^{+1.35}$
$M_{3.5}^{J/\psi}(^1S_0^{(8)}, ^3P_0^{(8)})$	$4.38 \pm 1.15_{-0.74}^{+1.52}$	$3.90 \pm 1.14_{-1.07}^{+1.46}$	$10.9 \pm 2.07_{-1.26}^{+2.79}$
$\langle \mathcal{O}_8^{\psi'}(^3S_1) \rangle$	$0.44 \pm 0.08_{-0.24}^{+0.43}$	$0.46 \pm 0.08_{-0.23}^{+0.41}$	$0.56 \pm 0.11_{-0.32}^{+0.54}$
$M_{3.5}^{\psi'}(^1S_0^{(8)}, ^3P_0^{(8)})$	$1.80 \pm 0.56_{-0.30}^{+0.62}$	$1.60 \pm 0.51_{-0.44}^{+0.60}$	$4.36 \pm 0.96_{-0.50}^{+1.11}$

Table 1: NRQCD matrix elements in  $10^{-2} \text{ GeV}^3$ . First error statistical, second error due to variation of scale. Ratio of  $\psi'$  to  $J/\psi$  fixed.

tributions in  $\alpha_s$  and also systematic effects inherent to NRQCD, such as the inaccurate treatment of energy conservation in the hadronization of the color octet quark pairs, modify the shape of the  $p_t$ -distribution, but are not reflected in the theoretical errors quoted in Tab. 1. In view of this, the values of  $M_{3.5}^{\psi}(^1S_0^{(8)}, ^3P_0^{(8)})$  should be considered with caution.

For  $\psi'$  production, an unconstrained fit of  $\langle \mathcal{O}_8^{\psi'}(^3S_1) \rangle$  and  $M_{3.5}^{\psi'}(^1S_0^{(8)}, ^3P_0^{(8)})$  leads to a value of the second parameter compatible with zero (with large error), or slightly negative for GRV and CTEQ4L PDFs. We conclude, that the present data does not allow a meaningful fit of this parameter. We therefore performed a combined fit of  $J/\psi$  and  $\psi'$  data under the (arguably plausible) assumption that the ratio  $M_{3.5}^{\psi}(^1S_0^{(8)}, ^3P_0^{(8)})/\langle \mathcal{O}_8^{\psi}(^3S_1) \rangle$  is the same for  $J/\psi$  and  $\psi'$ . The corresponding results for  $\psi'$  are also shown in Tab. 1.

We next consider charmonium polarization in the ( $s$ -channel) helicity frame ('recoil frame'). In this frame the polarization axis in the  $\psi$  rest frame is defined as the direction of the  $\psi$  three-momentum in the hadronic cms frame. Let  $P = p_p + p_{\bar{p}}$  be the sum of the initial hadron four-momenta and  $Q$  the  $\psi$  four-momentum. In the  $\psi$  rest frame  $\epsilon_L = \epsilon(\lambda = 0) = (0, -\vec{P}/|\vec{P}|)$ . The covariant expression reads

$$\epsilon_L(Q)_\mu = \frac{P \cdot Q}{\sqrt{(P \cdot Q)^2 - M^2 s}} \left( \frac{Q_\mu}{M} - \frac{M}{P \cdot Q} P_\mu \right), \quad (6)$$

where  $M$  is the quarkonium mass, taken to be  $2m_c$ , and  $\sqrt{s}$  the hadronic cms energy. We then obtain the longitudinal polarization fraction  $\xi =$

$p_t/\text{GeV}$	$a_L$	$b$	$c$	$c_L$
4	0.144	0.457	1.81	0.896
8	0.059	0.147	0.480	0.191
12	0.031	0.074	0.230	0.085
16	0.019	0.047	0.144	0.051
20	0.013	0.033	0.099	0.034
24	0.010	0.024	0.073	0.025

Table 2: Coefficients entering the longitudinal polarization fraction. Parameter specifications and pseudorapidity cut as for Fig. 1.

$d\sigma^{(\lambda=0)}/\sum_\lambda d\sigma^{(\lambda)}$ . The polar angular distribution in  $\psi \rightarrow l^+l^-$  decay is given by

$$\frac{d\Gamma}{d\cos\theta} \propto 1 + \alpha \cos^2\theta, \quad (7)$$

with  $\alpha = (1-3\xi)/(1+\xi)$  and  $\theta$  the angle between the lepton three-momentum in the  $\psi$  rest frame and the polarization axis, the  $\psi$  direction in the hadronic cms frame (lab frame). Note that in this frame scalar products like  $\epsilon_L(Q) \cdot k_1$  [see Eq. (4)] depend explicitly on parton momentum fractions  $x_i, x_j$  and can not be expressed in terms of partonic Mandelstam variables alone. For this reason, the partonic helicity amplitudes for the  $^3S_1^{(8)}$  channel computed in [7] can not be used for the present purpose.

In the large- $p_t$  limit, the  $^3S_1^{(8)}$  production channel yields transverse polarization, while the  $^1S_0^{(8)}$  and  $^3P_J^{(8)}$  channels both yield unpolarized quarkonia in this limit. However, for the longitudinally polarized cross section  $k$ , defined in Eq. (5), varies from 5.9 to 3.1 as  $p_t$  increases from 4 to 20 GeV, so that in the important region of low  $p_t$  a combination of  $\langle \mathcal{O}_8^\psi(^1S_0) \rangle$  and  $\langle \mathcal{O}_8^\psi(^3P_0) \rangle$  different from  $M_{3.5}^\psi(^1S_0^{(8)}, ^3P_0^{(8)})$  is required. We represent the longitudinal polarization fraction  $\xi$  as

$$\xi = \frac{a_L \langle \mathcal{O}_8^\psi(^3S_1) \rangle + b_L \langle \mathcal{O}_8^\psi(^1S_0) \rangle + c_L \langle \mathcal{O}_8^\psi(^3P_0) \rangle / m_c^2}{\langle \mathcal{O}_8^\psi(^3S_1) \rangle + b \langle \mathcal{O}_8^\psi(^1S_0) \rangle + c \langle \mathcal{O}_8^\psi(^3P_0) \rangle / m_c^2}. \quad (8)$$

The color singlet contribution is negligible. The coefficients  $a_L, c_L, b, c$  are shown in Tab. 2 as function of  $p_T$ . Note that  $b_L = b/3$  exactly. Fig. 3 displays  $\alpha$ , defined in Eq. (7) as function of  $p_t$ . The shaded band is obtained



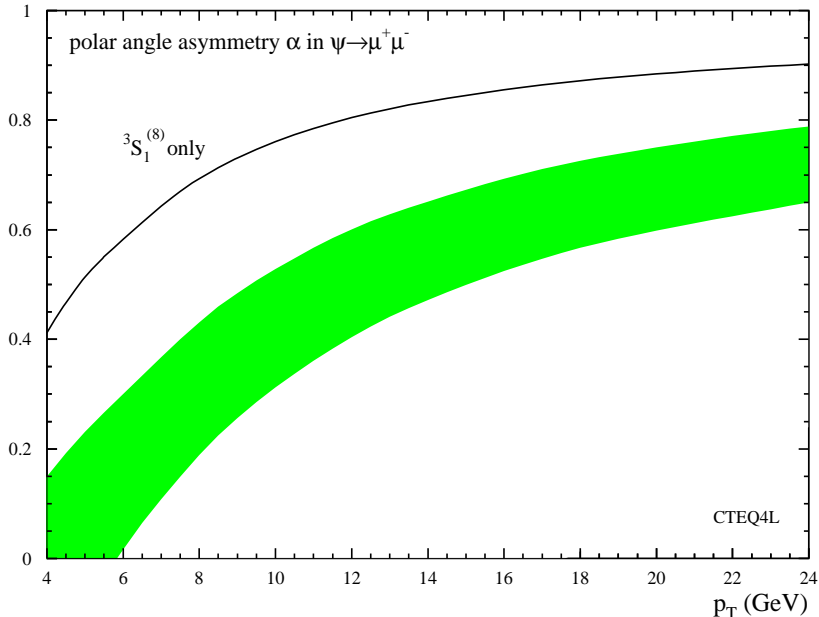


Figure 3:  $\alpha$  as a function of  $p_t$ . Parameter specifications as for Fig. 1. The band is obtained from Eq. (8) and the  $\mathcal{O}(\alpha_s^4)$  fragmentation contributions from [6] as described in the text. The solid curve is obtained with  $M_{3.5}^\psi(1S_0^{(8)}, 3P_0^{(8)}) = 0$  and shows the importance of this parameter for polarization. The band does not include theoretical uncertainties in the short-distance coefficients, Tab. 2.

as a combination of the uncertainty (statistical only) in the extraction of the NRQCD matrix elements [Tab. 1] and the limiting cases that either  $\langle \mathcal{O}_8^\psi(1S_0) \rangle$  or  $\langle \mathcal{O}_8^\psi(3P_0) \rangle$  is set to zero in the combination  $M_{3.5}^\psi(1S_0^{(8)}, 3P_0^{(8)})$ . Note that  $\alpha$  as a function of  $p_t$  is identical for  $J/\psi$  and  $\psi'$  production, because the ratios of NRQCD matrix elements for  $J/\psi$  and  $\psi'$  have been fixed. Thus, in comparing Fig. 3 with direct  $J/\psi$  polarization data,  $\psi'$  feed-down must be removed in addition to  $\chi$  feed-down. At low  $p_t \sim 5$  GeV, the theoretical prediction is compatible with unpolarized quarkonia. As  $p_t$  increases, the angular distribution becomes more and more anisotropic. At  $p_t \sim 15$  GeV, the fragmentation contributions of order  $\alpha_s^4$  computed in [6] become equally

important as the  $\alpha_s^3$  mechanisms computed here.<sup>2</sup> This second source of longitudinal polarization is included in the curves in Fig. 3.

In conclusion, we have evaluated the dominant sources of direct charmonium depolarization in  $p\bar{p}$  collisions at moderate transverse momentum. In the lower  $p_t$  range about 5 GeV, which, due to limitation in statistics, will be most relevant in the present Tevatron analysis, an essentially flat angular distribution is predicted, unless the  $\langle\mathcal{O}_8^\psi(^1S_0)\rangle$  and  $\langle\mathcal{O}_8^\psi(^3P_0)\rangle$  matrix elements are significantly smaller than their best fit values, obtained from the  $p_t$  distribution of the unpolarized cross section. With increasing  $p_t$ , the angular distribution is predicted to change rapidly due to the onset of substantial transverse polarization. Observation of a pattern as in Fig. 3 would provide support for the color octet charmonium production picture.

While this paper was in writing, charmonium polarization at moderate  $p_t$  has also been addressed by Leibovich [15]. Unfortunately, contrary to what is stated in the paper, he defines the polarization axis as the  $\psi$  direction in the partonic (rather than hadronic) cms frame. His results for the polar angle distribution can therefore not be used for comparison with Tevatron data.

We thank M. Mangano and V. Papadimitriou for discussions and for providing us with CDF data.

## References

- [1] G.T. Bodwin, E. Braaten and G.P. Lepage, Phys. Rev. **D51**, 1125 (1995)
- [2] E. Braaten and S. Fleming, Phys. Rev. Lett. **74**, 3327 (1995)
- [3] F. Abe *et al.*, Phys. Rev. Lett. **69**, 3704 (1992)
- [4] E. Braaten, S. Fleming and T.C. Yuan, OHSTPY-HEP-T-96-001 [hep-ph/9602374]; M. Beneke, SLAC-PUB-7173 [hep-ph/9605462], to appear in the Proceedings of the Second Workshop on Continuous Advances in QCD, Minneapolis, March 1996

---

<sup>2</sup>In Eq. (13) of [6] the factor 864 should be replaced by 96. The values of  $r_3$  in Tab. 1 of [6] must be multiplied by three.

- [5] P. Cho and M.B. Wise, Phys. Lett **B346**, 129 (1995)
- [6] M. Beneke and I.Z. Rothstein, Phys. Lett. **B372**, 157 (1996)
- [7] P. Cho and A.K. Leibovich, Phys. Rev. **D53**, 150 (1996); **D53**, 6203 (1996)
- [8] V. Papadimitriou, private communication
- [9] B. Guberina *et al.*, Nucl. Phys. **B174**, 317 (1980)
- [10] M. Beneke and I.Z. Rothstein, Phys. Rev. **D54**, 2005 (1996)
- [11] E. Braaten and Y.-Q. Chen, Phys. Rev. **D54**, 3216 (1996)
- [12] M.W. Bailey (for the CDF coll.), FERMILAB-CONF-96-235-E; A. Sansoni (for the CDF coll.), FERMILAB-CONF-96-221-E
- [13] M. Cacciari, M. Greco, M.L. Mangano, and A. Petrelli, Phys. Lett. **B356**, 560 (1995)
- [14] M. Glück, E. Reya and A. Vogt, Z. Phys. **C67**, 433 (1995); A.D. Martin, R.G. Roberts and W.J. Stirling, DTP/96/44 [hep-ph/9606345]; H.L. Lai *et al.*, MSUHEP-60426 [hep-ph/9606399]
- [15] A.K. Leibovich, CALT-68-2082 [hep-ph/9610381]